

DETECTING COMPLEX BUILDING SHAPES IN PANCHROMATIC SATELLITE IMAGES FOR DIGITAL ELEVATION MODEL ENHANCEMENT

B. Sirmacek, P. d'Angelo, P. Reinartz

German Aerospace Center (DLR), Remote Sensing Technology Institute
PO Box 1116, 82230, Wessling, Germany
(Beril.Sirmacek, Pablo.Angelo, Peter.Reinartz)@dlr.de

Commission VII

KEY WORDS: Urban Region, Modeling, Building Detection, DEM/DTM, Ikonos Images

ABSTRACT:

Since remote sensing field provides new sensors and techniques to accumulate data on urban region, three-dimensional representation of these regions gained much interest for various applications. Three-dimensional urban region representation can be used for detailed urban monitoring, change and damage detection purposes. In order to obtain three-dimensional representation, one of the easiest and cheapest way is to use Digital Elevation Models (DEMs) which are generated from very high resolution stereo satellite images using stereovision techniques. Unfortunately after applying the DEM generation process, we can not directly obtain three-dimensional urban region representation. In the DEM which is generated using only one stereo image pairs, generally noise, matching errors, and uncertainty on building wall locations are very high. These undesirable effects increase the complexity in the three-dimensional representation. Therefore, automatic DEM enhancement is an open and challenging problem.

In order to enhance DEM, herein we propose an approach based on building shape detection. We use DEM and orthorectified panchromatic Ikonos images of München to explain our method. After applying pre-processing to both DEM and Ikonos image, we apply local thresholding to DEM to detect approximate locations of high urban objects like buildings. In order to detect complex building shapes, we develop our previous rectangular shape detection (box-fitting) algorithm. Unfortunately, building shapes are very complex in our study region. We assume that shapes of these complex buildings can be detected by fitting small rectangles like a chain. Therefore, we divide detected buildings into elongated subparts. Then, we apply our previous rectangular shape detection algorithm to these subparts. In shape detection, we consider Canny edges of Ikonos image to fit rectangular boxes. After merging all detected rectangles, we detect shapes of even very complex building structures. Finally, using detected building shapes, we refine building edges in the DEM and smooth the noise on building rooftops. We believe that the implemented enhancement will not only provide better visual three-dimensional urban region representation, but also will lead to detailed change and damage investigations.

1 INTRODUCTION

Detection and three-dimensional reconstruction of buildings from remotely sensed images has been popular research topic in the recent years. Especially urban monitoring, damage assessment, disaster monitoring fields need to achieve realistic three-dimensional urban models. A rather new technology in this context is the Digital Elevation Model (DEM) generation based on stereo image matching principle using satellite data. Unfortunately, there are several problems in generated DEM. First, in most of the cases only two stereo satellite images are available. Regions which are occluded in one of these stereo images have no height value in DEM data. Interpolation techniques, which are used to fill these non-value regions, lead to lose sharpness in building edges. Generated DEM have limited resolution and raw DEM data may not represent buildings correctly. Generally these deficiencies are improved and three-dimensional buildings are reconstructed manually. For automation, some advanced processes are required to enhance the DEM. Therefore we believe that, intelligent fusion of computer vision techniques with photogrammetry can give better results in three-dimensional city interpretation.

In the previous work there is a wide variety of study on building detection and shape extraction from two-dimensional single satellite or aerial images. The earliest studies in this field generally depend on edge and line extraction (Krishnamachari and Chellappa, 1996, Irvin and McKeown, 1989, Davis, 1982). Unfortunately, these methods generally fail to detect buildings which have textured rooftops or which appear in complex environments. In order to cope with this problem, Saeedi and Zwick (Saeedi

and Zwick, 2008) combined edge information with graph based segmentation result of the region. To generalize building detection algorithm for different kind of environments, Sirmacek and Unsalan (Sirmacek and Unsalan, 2010, Sirmacek and Unsalan, 2009) developed local feature based robust, fast, and automatic approaches.

Many researchers developed more advanced methods to extract shapes of the detected buildings (Karantzas and Paragios, 2009, Cui et al., 2008, Benedek et al., 2009). Sirmacek and Unsalan (Sirmacek and Unsalan, 2008) developed a novel and fast method to detect shapes of rectangular buildings. Unfortunately, they could not detect other building shapes. In this study, we develop the same approach to detect shapes of very complex building structures.

As remote sensing technology and methods are developing, they provide new three-dimensional data such as DEM and LIDAR, and many researchers pay attention to building detection from this data. Haala et al. (Haala and Brenner, 1999) proposed a method to reconstruct building rooftops using surface normals extracted from DEM data. They assumed that building boundaries are detected previously. In a following study (Haala et al., 1998), they detected building boundaries automatically by classifying DEM and corresponding color image before applying their automatic rooftop reconstruction method. Brunn and Weidner (Brunn and Weidner, 1997) used surface normals on DEM to discriminate buildings and vegetation. After detecting buildings, they measured geometry of rooftops using surface normals and they interpolated polyhedral building descriptions to these structures.

Fradkin et al. (Fradkin et al., 1999) proposed segmentation based method to reconstruct three-dimensional models of dense urban areas. To this end, they used very high resolution color aerial images and DEM data. Canu et al. (Canu et al., 1996) used high resolution DEM to reconstruct three-dimensional buildings. First, they segmented DEM into homogeneous regions. Then, they interpolated flat surfaces on these regions. Ortner et al. (Ortner et al., 2002) used point process to model urban areas. They represented urban areas as interacting particles where each particle stands for an urban object. Preknowledge about building shapes is used to model these particles. Arefi et al. (Arefi et al., 2008) extracted above-ground objects from LIDAR data. Then, three-dimensional buildings are reconstructed by hierarchical fitting of minimum boundary rectangles (MBR) and RANSAC based straight line fitting algorithm. Tournaire et al. (Tournaire et al., 2010), developed a stochastic geometry based algorithm to detect building footprints from DEM data which has less than 1m resolution. They tried to fit rectangles on the buildings using an energy function and prior knowledge about buildings. To minimize the energy function, they used a Reversible Jump Monte Carlo Markov Chain (RJCMCMC) sampler coupled with a simulated annealing algorithm which leads to an optimal configuration of objects. In these studies, good results are achieved generally using very high resolution (more than 1 m. spatial resolution) DEMs which are generated from airborne data sets. However, enhancement of buildings in very low resolution urban DEM data which is generated from satellite images is still an open research problem.

In the literature, very few number of researchers worked on DEM enhancement. A considerable amount of these studies has been published on reducing errors in DEMs which belong to rural regions (Skarlatos and Georgopoulos, 2004, Ostrowski and He, 1989). For urban DEM enhancement Krauss and Reinartz (Reinartz and Krauss, 2010) developed image segmentation based algorithm. They obtained successful results in recovering occlusion errors in DEM generation. In a previous study, we have proposed an object detection based urban DEM enhancement system (Sirmacek et al., 2010). For this purpose, first we extracted possible building segments by thresholding DEM. Then we used Sirmacek and Unsalan's rectangular shape detection (box-fitting) algorithm to detect building shapes (Sirmacek and Unsalan, 2008). Finally, we used detected building shapes to sharpen building walls in DEM, and we also smoothed the noise in building rooftops. In this previous study, we could only detect and enhance rectangular buildings. Unfortunately, in most of the regions, buildings are in very complex shapes. In addition to that, all building shapes are different from each other, so it is not possible to search for a previously defined building shape. Therefore, more advanced shape detection algorithm is needed to apply our object detection based DEM enhancement method. To overcome this problem, herein we develop box-fitting algorithm in order to detect complex building shapes automatically. In Fig. 1, we represent overview of proposed algorithm for better understanding. Different from our previous object detection based urban DEM enhancement method, here we divide complex buildings into elongated shapes and detect chain of rectangles to extract their shapes. As a result, we can also enhance complex shaped buildings.

To test our method, and represent our results we use orthorectified panchromatic Ikonos satellite image, and automatically generated DEM of München city. Our DEMs are generated from single satellite image couples (d'Angelo et al., 2009). In the following sections, we explain algorithm steps in detail.

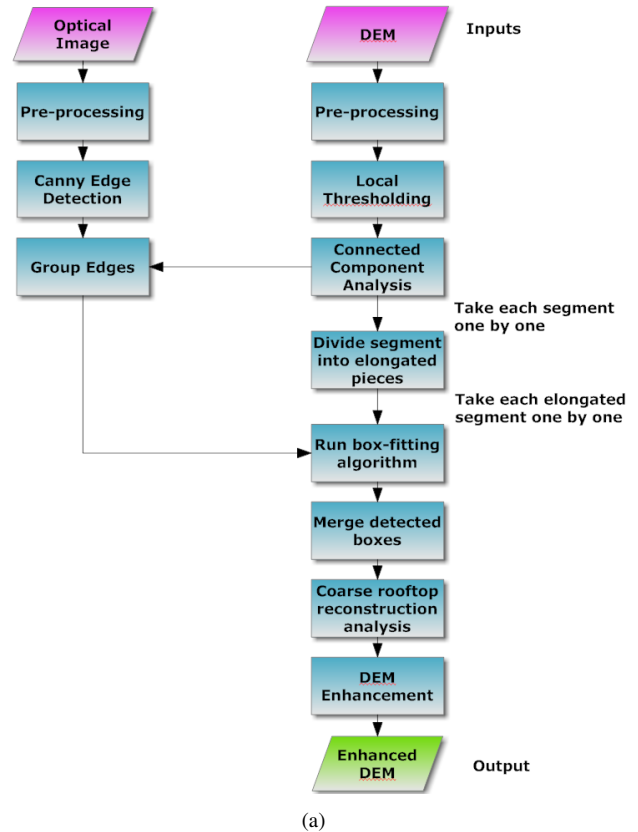


Figure 1: Overview of the proposed approach

2 PREPROCESS

Before starting to our building shape extraction and DEM enhancement processes, first we apply preprocessing to both panchromatic Ikonos image $I(x, y)$ and DEM $D(x, y)$.

In order to preprocess panchromatic data we benefit from bilateral filter. Bilateral filter performs a non-linear smoothing with preserving edge information (Tomasi and Manduci, 1998). In this way, we can eliminate noise and redundant details from the image without damaging edge information. Sirmacek and Unsalan (Sirmacek and Unsalan, 2009) provide an extensive explanation about usage of bilateral filter on panchromatic satellite images. We call bilaterally filtered satellite image as $I_b(x, y)$. In Fig. 2 (a), (b), and (c), we provide $I(x, y)$ panchromatic Ikonos test image, closer view of a sample building, and bilateral filtering result of the same building respectively.

Next, we prepare DEM for processing. DEM is a two-dimensional image where intensity values correspond to height information. It can be viewed as three-dimensional image, when intensity values are plotted as height information. Our DEM is unfortunately noisy and resolution is not enough to represent sharp building edges. In order to be able to detect building segments easily, we try to increase height difference between buildings and the ground surface. Histogram equalization method helps us to increase this difference (Acharya and Ray, 2005). We call this enhanced DEM as $D_e(x, y)$. In Fig. 2 (d) and (e), we provide original DEM and enhanced DEM of the sample building.

3 COMPLEX BUILDING SHAPE DETECTION

In the following subsections, we describe our complex building shape extraction algorithm step by step. Then, we will use these shapes for DEM enhancement.

3.1 Detecting Building Segments

Before extracting building shapes from panchromatic image, we first detect approximate building locations from enhanced DEM. If we had digital terrain model (DTM) of the region, we could use it to calculate normalized digital elevation model (nDEM). The difference between DEM and DTM gives nDEM (Sirmacek et al., 2010). In nDEM, ground height is referenced to zero, therefore it only provides information about building heights independent from the height of the terrain. If nDEM could be calculated, we could simply use a constant threshold value to obtain high objects in DEM which represents buildings. In our study, we segment high objects directly from DEM using local thresholding. Therefore, algorithm can be also used for regions which does not have DTM data.

We apply local thresholding to $D_e(x, y)$ and we obtain a binary image ($B_D(x, y)$) where high objects are labeled with 1 value. Since building edge quality in our DEM is not good, after applying local thresholding some of the close building segments can be extracted as conjoint segment. Therefore, we apply erosion to this binary image to separate connected building segments using a disk shaped structure with 2 pixels radius. Then, we apply labeling to $B_D(x, y)$ and obtain its connected components (Sonka et al., 1999). Here each connected component represents a building segment. If the size of a connected component is less than 500 pixels we discard it since these small regions generally correspond to tree clusters. Unfortunately, in this step we can not remove large tree clusters. We will work on discriminate vegetation in our future studies.

Boundaries of detected building segments do not directly indicate real building edges. Therefore after detecting building segments, in the next step we try to estimate real shapes of buildings using more advanced shape detection algorithm.

3.2 Fitting Chain of Boxes to Extract Building Shape

In a previous study Sirmacek and Unsalan (Sirmacek and Unsalan, 2008) proposed an automatic rectangular shape approximation approach (called box-fitting). After detecting a seed-point (approximate building center) on building rooftop, they grew a virtual box based on an energy criteria. In Fig. 3, a demonstration of box-fitting algorithm. The first image shows Canny edges of building the sub-image. In the second image, a virtual box is inserted to the approximate building center, and its edges are swept outwards. In the last image, fitted box shape is represented. In previous study, we used the same approach to detect rectangular building shapes (Sirmacek et al., 2010) in panchromatic satellite images. We used detected rectangular shapes to improve DEM. Unfortunately, we could not detect complex building shapes.

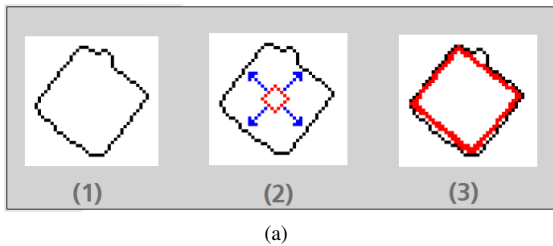


Figure 3: Demonstration of box-fitting approach

In this study, we propose a new method to improve box-fitting approach to detect complex building shapes. To this end, we first divide detected building segments into elongated pieces. Then we use our box-fitting algorithm to detect rectangular shape in this

region. After running box-fitting algorithm on each elongated segment, we obtain complex building shapes as a chain of rectangles. We propose an easy method to divide building into elongated pieces. First we extract skeleton of the building segment using $B_D(x, y)$ (Sonka et al., 1999). Then, we detect junctions of this skeleton. Junction is defined as one pixel which have more than two pixels in the neighborhood. We divide skeleton into pieces from junction locations. If Euclidean distance between two junctions are larger than 20 pixels, we divide the skeleton between these two junctions into 20 pixel length pieces. We assume coordinates of mass centers of divided skeleton pieces as our seed-point locations ((x_s, y_s)).

To fit rectangular shapes into each (x_s, y_s) location, we locate a $[w \times w]$ size window on this building center. We assume w as equal to two times of skeleton piece length. Then we grow the virtual box on each (x_s, y_s) location until the virtual box best fits to the Canny edges of the building. Box-fitting method discards edges out of window to deal only with candidate building edges and to decrease the number of unnecessary edges. After our virtual box stops growing, we calculate the energy E_θ . The energy of the detected box shape is defined as the sum of minimum distance between virtual building edge pixels and real building edge pixels in perpendicular direction as given below;

$$E_\theta = \sum_{i=1}^n \min(\text{sqr}t((x_v(i) - x_e(j))^2 - (y_v(i) - y_e(j))^2)) \quad (1)$$

Here, E_θ is the calculated energy in θ direction. $(x_v(i), y_v(i))$ represent coordinates for i th pixel on the edges of the virtual box shape. $(x_e(j), y_e(j))$ represents the j th pixel on the real building edges. For same seed-point, we put an initial virtual box and start growing again for all $\theta \in [0, \pi/6, \pi/3, \pi/2, 2\pi/3, \dots, 2\pi]$ angles. As we increase step sizes here, we can obtain more accurate approximations, however we need more computation time. After calculating E_θ for $\theta \in [0, \pi/6, \pi/3, \pi/2, 2\pi/3, \dots, 2\pi]$ angles, we pick the estimated box which has smallest E_θ energy as detected building shape. Since buildings are generally in rectangular shapes, it makes sense to extract rectangular shapes on buildings. Main advantage of using box-fitting approach is that approximate building shape still can be found even the building edges are not well-determined, or even if there is not a closed shape. However, other region growing algorithms fail to extract an object shape in these cases.

In Fig. 2 (f), we represent detected boxes for our sample building. Next, we describe how to detect building shape from chain of boxes.

3.3 Shape Refinement

After detecting chain of boxes using Canny edges of panchromatic satellite image, we apply a boundary refinement step to fit into building edges better, and also to smooth the discontinuity of connected boxes. First, we fill inside of detected boxes with 1 value. We apply dilation and erosion respectively to the detected boxes, using a disk shaped structure with radius 2. After this operation all detected boxes can be fused, but discontinuity between adjacent box corners can not be corrected. After merging boxes, obtained building shape can be seen in Fig. 2 (g). Discontinuity between adjacent boxes cause fluctuations on some parts of the detected shape. To correct building shape, we apply line fitting. First, we choose an arbitrary point on building border. Then, in clockwise direction we divide this border into 20 pixel

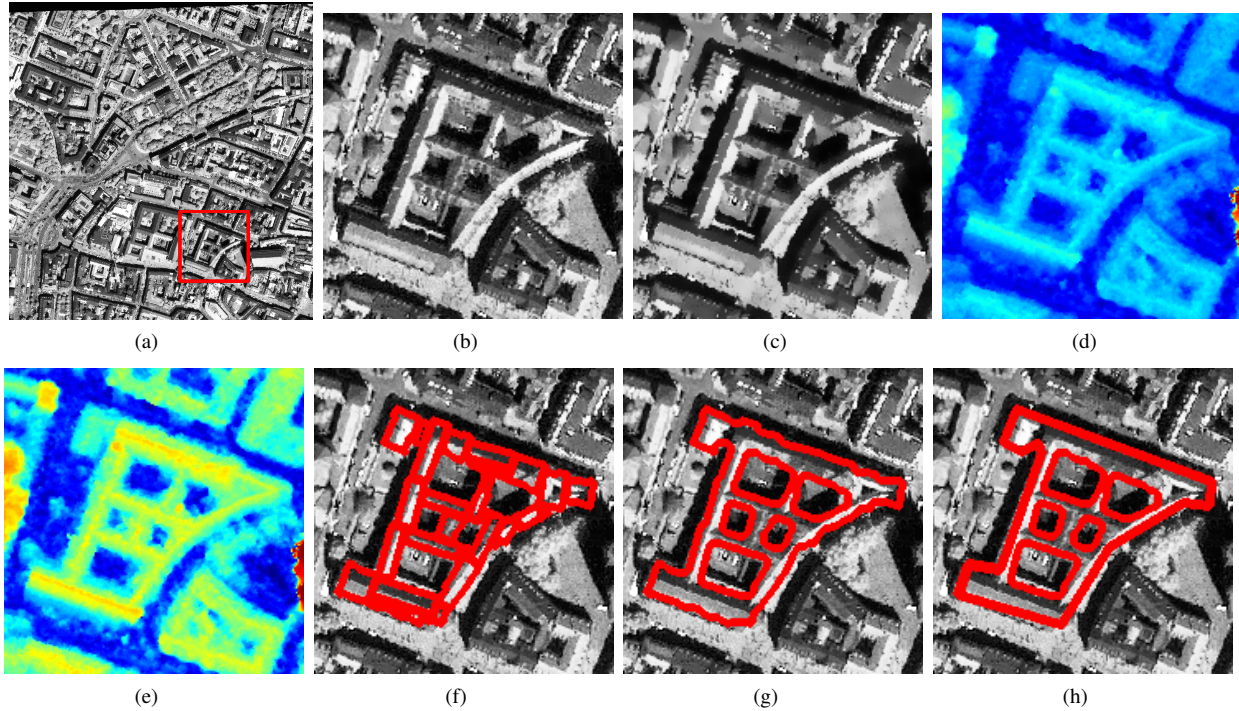


Figure 2: (a) Orthorectified panchromatic Ikonos test image of the study region (sample building is labeled with red borders), (b) Closer view of sample building, (c) Bilaterally filtered result, (d) Original DEM data of sample building, (e) DEM data after applying pre-processing, (f) Detected chain of boxes, (g) Merged boxes, (h) Refined building shape.

length pieces. We find the best fitting line into these pieces. After merging detected lines, we obtain more clear building shape. Detected shape for our sample building can be seen in Fig. 2 (h). In the next step, we use this shape to insert sharp building edges to DEM data.

4 DEM ENHANCEMENT

In DEM data we should enhance both building shapes and their height information. To visualize our enhancement process, we take a slice of our sample building in Fig. 4. In Fig. 4 (a), slide is given with red line. In Fig. 4 (b), three-dimensional view of DEM ($D(x, y)$) is given. For better visualization, we set the region into zero value which has also zero value in $B_D(x, y)$. Therefore, we can only see height information that belongs to building segment. Unsharp building shape and noisy rooftop can be seen in this three-dimensional view. In Fig. 4, we plot the values of $D(x, y)$ on taken slide. Diffused building walls, and noisy height information can be seen better on this plot.

In order to enhance $D(x, y)$, first we insert sharp edges on the locations where building borders are detected. After that, we analyze the rooftop for enhancing height information. To do that, we only smooth $D(x, y)$ with median filter. For now, we do not reconstruct detailed rooftop, but we use intelligent method to choose size of median filter. We analyze discontinuities in $D(x, y)$ by checking gradient magnitudes. To find gradient magnitudes, we use smoothed gradient filters in x and y directions as below,

$$g_x(x, y) = \frac{-x}{2\pi} \exp\left(-\frac{x^2 + y^2}{2\sigma^2}\right) \quad (2)$$

$$g_y(x, y) = \frac{-y}{2\pi} \exp\left(-\frac{x^2 + y^2}{2\sigma^2}\right) \quad (3)$$

where σ is the smoothing parameter and equal to 0.5. Although method is fairly robust to this parameter, one may need to adjust it according to the resolution of DEM. We calculate the smoothed gradients for $D(x, y)$ as,

$$d_x(x, y) = g_x(x, y) * D(x, y) \quad (4)$$

$$d_y(x, y) = g_y(x, y) * D(x, y) \quad (5)$$

where $*$ stands for a two-dimensional convolution operation. We calculate gradient magnitudes of image as,

$$G(x, y) = \sqrt{d_x(x, y)^2 + d_y(x, y)^2} \quad (6)$$

If a pixel in $G(x, y)$ has a higher value than t_d , we assume there is a significant discontinuity. Here, t_d threshold value is obtained by Otsu's automatic thresholding approach (Otsu, 1979). We control if there is a significant discontinuity on detected building rooftop. If there is a significant discontinuity, we assume that, there can be an object on building rooftop. In order to not smooth this object, we choose a smaller median filter window size as 3×3 . Otherwise, we use 9×9 size window, to remove noise and redundant information on building rooftop. In Fig. 4 (d) and (e), reconstructed three-dimensional building and its profile on the same slice are given. Improvement on building shape is significant. We will work on more detailed rooftop reconstruction in our future studies.

5 EXPERIMENTAL RESULTS

To test the performance of our method, we study on München city which includes very complex building structures. We use DEM

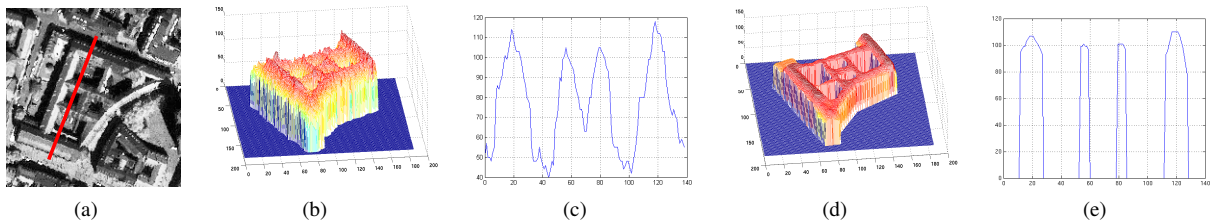


Figure 4: (a) Sample building and taken slice (b) Original DEM values of extracted building region (c) Values of the original DEM along the slice, (d) Enhanced DEM (e) Values of the enhanced DEM along the slice

which is generated from stereo Ikonos images using the DEM generation method of d'Angelo et al. (Reinartz and Krauss, 2010). We also use orthorectified panchromatic Ikonos image of the corresponding region.

We presented our shape detection and DEM enhancement results on Fig. 2(h), and Fig. 4(d) respectively. In Fig. 5, we represent result of our complex shape detection algorithm on different building structures. Next, we analyze performance of our proposed method on sample building to give a sight to possible readers.

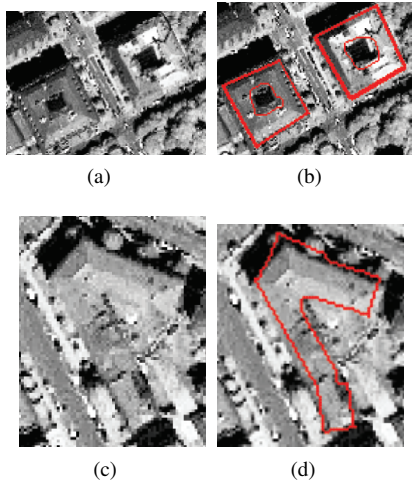


Figure 5: Examples for extracted complex building shapes

We pick our test building (given in Fig. 2 (b)) to evaluate performance of our complex shape detection method. To analyze performance we consider two measures; shape accuracy (p_1) and height accuracy (p_2). First, we start with measuring shape accuracy of the shape approximation (box-fitting) approach. We use the method used by Ruether et al. (Ruether et al., 2002) to measure the shape accuracy. For a $[m \times n]$ size test image shape accuracy performance (p_1) is calculated as follows,

$$p_1 = \left(\frac{\sum_{x=1}^m \sum_{y=1}^n |B_f(x, y) - B_{gth}(x, y)|}{\sum_{x=1}^m \sum_{y=1}^n B_{gth}(x, y)} \right) \times 100 \quad (7)$$

in this equation $B_f(x, y)$ is the binary image which is obtained by assigning value 1 to detected rooftop region. B_{gth} is the binary groundtruth shape mask that we labeled buildings as '1' and other regions as '0' manually. We calculate p_1 value as 85,06% for sample complex building structure.

We finally analyze computation time needed for our method. We use our sample complex building to calculate computation times. We obtain timings using an Intel Core2Quad 2.66GHz PC and

Matlab coding environment. Segmenting building regions from DEM data requires only 0.30 seconds. The longest computation time is needed for shape detection step. For sample building, shape detection step requires 152 seconds.

In this step, timing directly depends on the complexity and size of the building. As the complexity and size of the building increase, the shape detection method needs more computation time. However, this module can run faster if it is coded in C. Finally, enhancing building shapes in DEM requires 12.52 seconds. Consequently, running our proposed DEM enhancement method on complex building requires 164.82 seconds. The computation time of the proposed DEM enhancement method is better than previous systems in the literature.

6 CONCLUSIONS

Automatic generation of three-dimensional urban regions can be an innovative way for providing geometric data for varieties of applications such as disaster management, military situations, and urban planning. Therefore, reliable and consistent generation of three-dimensional urban maps is crucial. Developing remote sensing technology and methods offer new and cheap approaches such as DEM generation based on stereo satellite image matching principle. Unfortunately, DEM is not directly suitable for three-dimensional representation. DEM generation errors, noise, and smooth building walls as a result of occlusion effect make raw DEM useless for three-dimensional visualization. Advanced methods are needed to improve this DEM.

Herein, we introduced a novel method for automatic DEM enhancement based on building shape extraction. First, we found the building segments by applying local thresholding the DEM. Then, we used Canny edges of corresponding panchromatic image for shape extraction. We developed rectangular shape detection (box-fitting) algorithm to detect very complex building structures. Extracted building shapes helped us to sharpen building edges, and to smooth rooftop noise in the DEM. After tests on München city data which includes very complex building structures. Comparing with studies presented in the literature, we can conclude that our proposed urban DEM enhancement method is fast and reliable even in complex urban regions. The proposed automatic method will decrease operator work-loads in three-dimensional reconstruction of urban areas. In addition to that, we believe that the proposed method will be of use for detailed urban monitoring, damage and change detection systems. In our future study, we will try to add detailed rooftop reconstruction to building models.

REFERENCES

Acharya, T. and Ray, A., 2005. Image processing: Principles and applications. Wiley-Interscience.

- Arefi, H., Engels, J., Hahn, M. and Mayer, H., 2008. Levels of detail in 3d building reconstruction from lidar data. In Proceedings of International Archives of Photogrammetry, Remote Sensing, and Spatial Information Sciences 37, pp. 485–490.
- Benedek, C., Descombes, X. and Zerubia, J., 2009. Building extraction and change detection in multitemporal aerial and satellite images in a joint stochastic approach. INRIA, Paris, France, Tech. Rep.
- Brunn, A. and Weidner, U., 1997. Extracting buildings from digital surface models. In Proceedings of International Archives of Photogrammetry, Remote Sensing, and Spatial Information Sciences.
- Canu, D., Gambotto, J. and Sirat, J., 1996. Reconstruction of building from multiple high resolution images. In Proceedings of International Conference on Image Processing.
- Cui, S., Yan, Q. and Liu, Z., 2008. Right-angle building extraction based on graph-search algorithm. International Workshop on Earth Observation and Remote Sensing Applications, EORSA 2008 1, pp. 1–7.
- d'Angelo, P., Schwind, P., Krauss, T., Barner, F. and Reinartz, P., 2009. Automated dsm based georeferencing of cartosat-1 stereo scenes. In Proceedings of International Archives of Photogrammetry, Remote Sensing, and Spatial Information Sciences.
- Davis, L., 1982. Hierarchical generalized hough transforms and line-segment based generalized hough transforms. Pattern Recognition 15 (4), pp. 277–285.
- Fradkin, M., Roux, M., Maitre, H. and Leloglu, U., 1999. Surface reconstruction from multiple aerial images in dense urban areas. In Proceedings of IEEE Computer Vision and Pattern Recognition 2, pp. 262–26.
- Haala, N. and Brenner, C., 1999. Extraction of buildings and trees in urban environments. ISPRS Journal of Photogrammetry and Remote Sensing 54, pp. 130–137.
- Haala, N., Brenner, C. and Anders, K., 1998. 3d urban gis from laser altimeter and 2d map data. In Proceedings of International Archives of Photogrammetry, Remote Sensing, and Spatial Information Sciences 32, pp. 339–346.
- Irvin, R. and McKeown, D., 1989. Methods for exploiting the relationship between buildings and their shadows in aerial imagery. IEEE Transactions on systems, Man and Cybernetics 19 (6), pp. 1564–1575.
- Karantzas, K. and Paragios, N., 2009. Recognition-driven two-dimensional competing priors toward automatic and accurate building detection. IEEE Transactions on Geoscience and Remote Sensing 47 (1), pp. 133–144.
- Krishnamachari, S. and Chellappa, R., 1996. Delineating buildings by grouping lines with mrfs. IEEE Transactions on Image Processing 5 (1), pp. 164–168.
- Ortner, M., Descombes, X. and Zerubia, J., 2002. Building extraction from digital elevation models. INRIA Research Report.
- Ostrowski, J. and He, D., 1989. Error correction of digital elevation models produced by automatic matching of digital stereo images. In Proceedings of International Geoscience and Remote Sensing Symposium (IGARSS) 2, pp. 446–449.
- Otsu, N., 1979. A threshold selection method from gray-level histograms. IEEE Transactions on SMC 9, pp. 62–66.
- Reinartz, P. and Krauss, T., 2010. Enhancement of dense urban digital surface models from vhr optical satellite stereo data by pre-segmentation and object detection. In Proceedings of Canadian Geomatics Conference, CGC'2010.
- Ruether, H., Martine, H. M. and Mtaló, E., 2002. Application of snakes and dynamic programming optimisation technique in modelling of buildings in informal settlement areas. ISPRS Journal of Photogrammetry and Remote Sensing 56 (4), pp. 269–282.
- Saeedi, P. and Zwick, H., 2008. Automatic building detection in aerial and satellite images. International Conference on Control, Automation, Robotics and Vision, ICARCV 2008, Hanoi, Vietnam 1, pp. 623–629.
- Sirmacek, B. and Unsalan, C., 2008. Building detection from aerial imagery using invariant color features and shadow information. International Symposium on Computer and Information Sciences ISCIS'2008, Istanbul, Turkey.
- Sirmacek, B. and Unsalan, C., 2009. Urban area and building detection using sift keypoints and graph theory. IEEE Transactions on Geoscience and Remote Sensing 47 (4), pp. 1156–1167.
- Sirmacek, B. and Unsalan, C., 2010. A probabilistic framework to detect buildings in aerial and satellite images. IEEE Transactions on Geoscience and Remote Sensing pp. –.
- Sirmacek, B., d'Angelo, P., Krauss, T. and Reinartz, P., 2010. Enhancing urban digital elevation models using automated computer vision techniques. ISPRS Commission VII Symposium, Vienna, Austria.
- Skarlatos, D. and Georgopoulos, A., 2004. Automating the checking and correcting of dems without reference data. In Proceedings of International Archives of Photogrammetry, Remote Sensing, and Spatial Information Sciences 35, Part B2, pp. 553–558.
- Sonka, M., Hlavac, V. and Boyle, R., 1999. Image processing, analysis and machine vision. PWS Publications, Pacific Grove, CA, second edn.
- Tomasi, C. and Manduci, R., 1998. Bilateral filtering for gray and color images. In Proceedings of International Conference on Computer Vision 1), pp. 839–846.
- Tournaire, O., Bredif, M., Boldo, D. and Durupt, M., 2010. An efficient stochastic approach for building footprint extraction from digital elevation models. ISPRS Journal of Photogrammetry and Remote Sensing 65 (4), pp. 317–327.